AIAA JOURNAL
Vol. 42, No. 2, February 2004

Computing Existence and Stability of Capillary Surfaces Using Surface Evolver

Steven H. Collicott*
Purdue University, West Lafayette, Indiana 47907-2015
and
Mark M. Weislogel†
Portland State University, Portland, Oregon 97207-0751

In response to the growing need for design specific solutions predicting interface existence and stability in an ever-increasing number of low-gravity fluids systems applications, K. A. Brakke's surface evolver (SE) algorithm, developed to compute complex interfacial static equilibria, is demonstrated to successfully compute critical contact angles and the onset of the Rayleigh–Taylor instability. SE is first benchmarked against limited available analytical solutions and then extended to solve the specific problem of stability in rectangular containers where the effect of discontinuous boundaries and wetting play a dramatic role. In this new light SE is shown to serve the purposes of an equilibrium interface solver, critical contact angle solver, and a capillary stability solver. Concerning the latter and in contrast to other numerical dynamic stability schemes, the significantly increased time efficiency and accuracy of the approach for capillary stability problems of significant geometric complexity argue for the use of SE as a valuable tool for spacecraft systems design.

Nomenclature

a	=	half-length of rectangular container
B	=	bond number ($\rho g R^2/\sigma$)
B_{cr}	=	critical Bond number identifying stability limits
b	=	half-width of rectangular container
C_1, C_2	=	fit coefficients for circular annulus
D_1, D_2	=	generic fit coefficients
g	=	acceleration field strength, that is, gravitational acceleration
m, n	=	integer indices
R	=	characteristic length scale
R_i	=	inner radius for circular annulus
R_o	=	outer radius for circular annulus
x, y	=	transverse coordinates in a cylinder
z	=	axial coordinates in a cylinder
α	=	half the angle of an interior corner of container
θ	=	contact (wetting) angle
θ_{cr}	=	critical contact angle
λ	=	disturbance wavelength
ρ	=	density difference across interface
σ	=	interfacial tension

I. Introduction

MULTIPHASE fluids systems in the weightlessness of space flight often rely on the presence of specific capillary free-surface positions, topologies, or shapes to function properly. Such fluids systems for orbital, drop tower, or other weightless environments might similarly depend on successful transition of a liquid–gas pair from high-g to low-g conditions.

The critical contact angle theory developed by Concus and Finn[1] describes conditions that separate two distinct types of liquid–gas interface solutions in a class of containers and presents a solution method for determining the critical contact angle or Concus–Finn angle. Others have observed the effect in a specific geometry or added to the understanding of it.[2–5] Additionally, classical capillary instability theory describes a maximum adverse acceleration (critical Bond number) for which an equilibrium interface is stable. The critical contact angle, if it exists, and the critical Bond number for capillary instability in a cylinder are two distinct topics. Critical contact angle analysis determines the conditions for existence of solutions of one topology. Capillary instability analysis begins with a stable static equilibrium solution for a free surface and seeks limits on acceleration, size, density, and surface tension expressed as a critical Bond number for which that equilibrium is stable. The use of the surface evolver (SE) code to solve for critical contact angles is discussed first with solutions for critical Bond numbers in capillary instability problems discussed second.

II. Critical Contact Angle

Weightlessness is not a requirement for the critical contact angle theory to apply, but the theory is especially useful as a design tool for such conditions and the manifestations of the results on surface shape are greatest in weightlessness. This type of analysis has been performed for a variety of geometries, including cylinders of fairly general cross section, including rectangles with blunted corners,[6] annuli,[7] corners of differing contact angles,[8] and a number of less obvious shapes.[6,9] Experiments have confirmed the theory in orbit[10] and in drop towers.[11]

Concus and Finn considered cylindrical containers and corners therein and addressed the question of the existence of a solution for the free surface shape $z = f(x, y)$ that covers one end (the "bottom") and is single valued and finite height (in z) at all (x, y) in the cross section and on the perimeter. If such a solution exists, then in the case of a zero-g fluids experiment one can see for a smooth transition from one-g to zero-g that the liquid initially in the bottom of the cylinder as shown in Fig. 1a will remain in the bottom, with a new interface shape as shown in Fig 1b. If the contact angle is below a critical value, here defined as the Concus–Finn angle, and $g = 0$, a single-valued finite-height solution does not exist as the fluid rises in the critically wetted corners to an infinite height (Fig. 1c) or, in any real container, to and perhaps around the upper perimeter of the container. Note that for sharp interior corners the increase in meniscus height to infinity as the contact angle is decreased below the Concus–Finn angle is discontinuous.

The Concus–Finn angle divides the existence and nonexistence of an assumed form of the interface (see Ref. 12 for a descriptive

Received 22 December 2001; revision received 10 September 2002; accepted for publication 14 July 2003.

*Associate Professor, Aerospace Sciences Laboratory, 1375 Aviation Drive. Associate Fellow AIAA.
†Associate Professor, Mechanical Engineering.

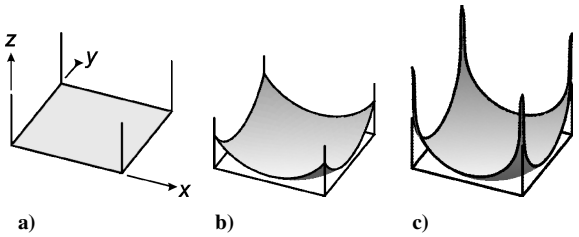

Fig. 1 Interfaces in a right square cylinder: a) SE starting geometry, b) 0 *g* with 50-deg contact angle, and c) 0 *g* with 42-deg contact angle and not converged. The four vertical lines in the corners illustrate the locations of the corners of infinite *z* extent.

overview). It is not a condition of stability for the interface. Analysis to solve for the Concus–Finn angle for a particular wetting condition and container geometry relies on classical (macroscopic) assumptions of surface tension and fixed contact angle and thus is a powerful demonstration of the validity of applying those two simple concepts (and presumably their SE representations) to solving problems and designing containers for low-*g* fluids needs. Note that stability of the SE algorithm about a solution, such as a liquid–vapor interface, is addressed by Brakke.[13] Application of SE to capillary instability problems, including validation against classical analytical solutions, is addressed below.

The practical value of the Concus–Finn critical contact-angle analysis motivates research into computing such wetting geometries through numerical models of the fluids. Brakke's SE[13,14] is a powerful numerical tool to accomplish such tasks and is based on energy minimization with a discretized free surface. SE has proven very useful for low-g fluids analysis where three-dimensional finite volume-of-fluid and other codes perform relatively poorly.[15–17] Through use of SE, it is hoped that the Concus–Finn analysis can be extended to important, nonidealized surface topologies of increased complexity that might not be amenable to efficient analysis. Furthermore, demonstration that a numerical model already in use for spacecraft and other low-*g* fluid systems captures the physics described by Concus–Finn theory strengthens the usefulness of designs developed with the SE code.

A first step in applying SE to compute the critical contact angles is to develop and validate a modeling procedure for known geometries. This process differs from using SE to compute example surface shapes for various contact angles. The question is not one of how well SE is designed, but whether a discrete numerical model of the continuous interfaces accurately captures the critical physical behavior. The first portion of this paper reports the validation of a method using SE for computing Concus–Finn critical contact angles and presents results illustrating grid convergence and finite precision.

A. Method: Critical Contact Angle

For cylinders of general section, SE is set up to model a free surface that spans the cross section above a fixed volume of liquid. The contact-angle boundary condition is set in SE with constraint energy integrals on the cylinder walls. The maximum height of the free surface is used to assess the existence of a single-valued finite-height solution for $f(x, y)$. The finite run time of a numerical model prevents computation of an infinite height interface. Thus, a practical method to discriminate between finite and infinite height solutions is required. Development of this method is one product of this research.

The SE model begins as a flat surface at $z = 0$, as shown for a square cylinder in Fig. 1a. As the Concus–Finn analysis does not depend on depth of the liquid above the bottom of cylinder, $z = 0$ can be placed at a convenient position. An example converged finite-height solution is shown in Fig. 1b, and an infinite-height solution (necessarily not converged) is shown in Fig. 1c.

To reliably iterate from the starting geometry of very few faces to the final geometry that is either a converged finite-height solution of thousands of faces or a solution that grows in z with each iteration requires a repeatable method. In this research SE commands are scripted to automate the surface evolution in a repeatable manner. This method is efficient for the researcher as SE can be left alone to compute a given case without interaction.

Three tests are reported: sufficient iteration count, grid convergence, and curved wall performance. Iteration count is examined in a square with two different contact angles on the walls meeting at the corner.[8] Grid convergence is assessed in square cylinders with equal contact angles on all four walls. Curved wall performance is examined because the straight edges of SE faces cannot conform exactly to the curve, and thus discretization errors are expected to be most substantial in this geometry.

An iteration count criterion is necessary to assess when one has iterated sufficiently long to determine that a solution is converging to a finite height or if the solution is merely growing in height in continued small steps. Such an assessment is obvious in simple geometries, yet a proven method is sought to permit intelligent assessment as computational time increases with increasing numbers of faces or for efficiently analyzing geometries that are more complex. For example, when the ratio of largest to smallest length scale in the cross section increases then the number of faces required to resolve the small length scale over the large area, while maintaining a 10-fold limit on the range of edge lengths, increases rapidly.

B. Critical Contact-Angle Results

Figure 2 shows results of the iteration count assessment for the 90-deg corners in a square cylinder with edge length of 2 and 4096 faces in the finite-height geometry. For a contact angle of 45 deg held constant on one wall, the critical contact angle predicted by Concus–Finn theory for the second wall is also 45 deg. In Fig. 2 the maximum height of the solution at each iteration is plotted for four different contact angles on the second wall. The convergence of two larger contact angle solutions compared with the continued growth of the two lesser contact angle solutions is evident, even as early as an iteration count equal to the number of initial faces. Figure 3 shows the change in height Δz per iteration for the same computations as in Fig. 2. Note that the curves for the large contact angles, for which there exists a finite-height single-valued interface, have a negative dip and are very close to zero after an iteration count equal to the initial face count (4096 here). It is doubtful that the negative dip is reliable for discriminating between contact angles greater than and less than the critical contact angle.

Grid convergence is assessed through attempts to bound the Concus–Finn critical contact angle in a square cylinder where all four sides have the same contact angle. Concus–Finn theory predicts a discontinuity in the plot of height vs contact angle in this geometry. (Other geometries might be continuous in this regard.) Results (Fig. 4) show that coarser grids (64 or 256 faces) produce ambiguous bounds such that a critical contact angle can not be determined within several degrees. Finer grids in this example, such as 1024 faces and higher, produce increasingly fine resolution of the critical contact angle. Note that all grids produce a finite-height

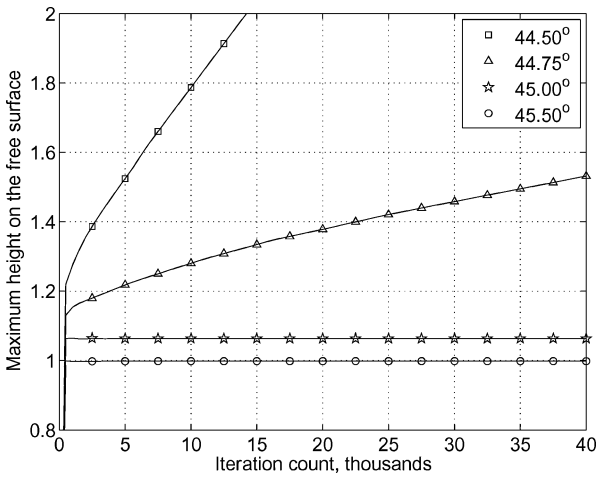

Fig. 2 Height of interface vs iteration count for 4096 initial faces.

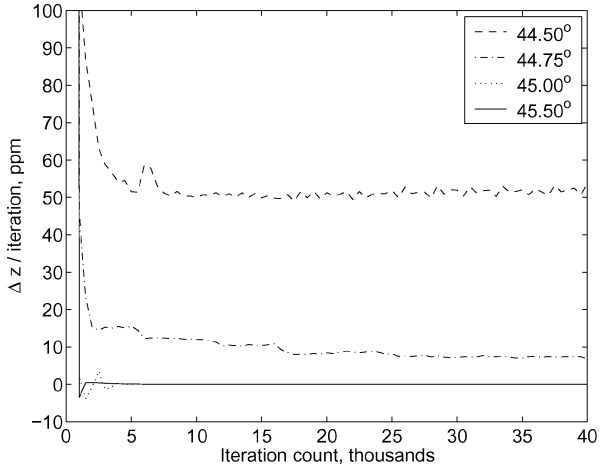

Fig. 3 Change in the height of the interface per iteration, parts per million, for the case of 4096 initial faces in a square cylinder of length two on a side.

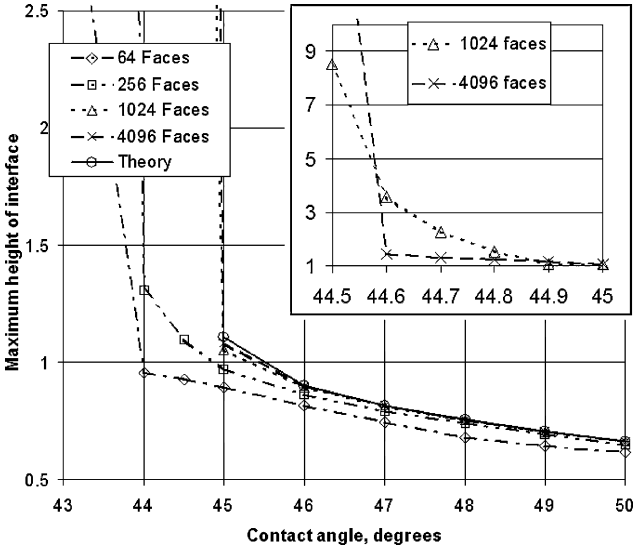

Fig. 4 Grid-convergence study. The 1024 line extends up to $z \approx 8.5$ at 44.5 deg and the 4096 line to $z \approx 18$ at 44.5 deg. The inset plot shows details of the 1024 and 4096 curves between 44.5 and 45 deg.

solution at 45-deg contact angle, consistent with theory, indicating that the bounds determined from computations will give lower critical contact angle for the discretized surface than the continuous surface.

The rounded rectangle analysis[6] shows how the finite corner bluntness in any manufactured container reduces critical contact angle from the sharp-corner result. The SE solutions are simple to distinguish as finite height or not, except at the largest bluntness radii where the critical contact angle approaches zero. This is consistent with the preceding grid-convergence study, which shows that a discretized surface has lower critical contact angle than the continuous surface. Another source of the inaccuracy might be that the gap constant in the SE model that compensates for the surface area between the straight face edge and the curved wall needs to be increased to prevent bunching of vertices (zero-length edges) on the curved wall as the contact angle is reduced. Regardless, the performance is excellent for Concus–Finn angles away from 0 deg (Fig. 5).

III. Capillary Instability

Since the inception of space flight, a number of studies have been conducted to identify the stability limits of large capillary surfaces to unfavorable disturbances (accelerations). The motivation for such investigations is generally to obtain design characteristics and performance limits for in-space fluids management systems. For example, it is essential to understand the potentially destabilizing effects of aerodynamic drag or thruster firing on the liquid fuel in a partially filled tank of a spacecraft. Other destabilizing forces include a host of operational disturbances caused by orbital maneuvers, spin stabilization, docking, even astronaut kickoff and exercise loads. Many terrestrial applications can be cited as well.

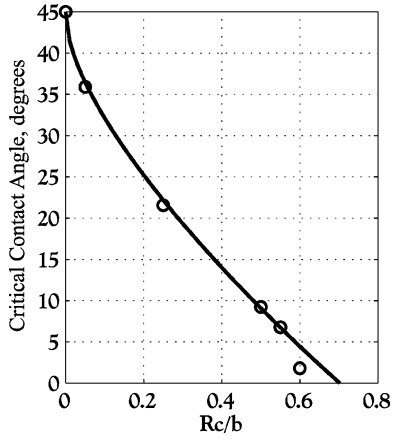

Fig. 5 Critical contact angle in a rounded rectangle of 2:1 aspect ratio: ——, Concus–Finn results[6]; points are from use of SE.

A brief review focused on a restricted set of container geometries for which solutions of interfacial instability of the Rayleigh–Taylor type are offered in the literature is provided. In response to the growing need for design specific solutions in an ever-increasing number of low-g fluids systems applications,[18] SE,[‡] developed to compute complex interfacial static equilibria but not dynamics of fluids, is demonstrated to successfully compute the onset of the Rayleigh–Taylor instability. SE is first benchmarked against available analytical solutions and then, as proof of its utility, is applied to solve the valuable problem of stability in rectangular containers where the effect of discontinuous boundaries and wetting play a dramatic role.

Surface-tension forces dominate fluid interface behavior for low-Bond-number systems, $B \ll 1$, where $B = \rho g R^2/\sigma$. As B is increased toward $\mathcal{O}(1)$, however, a critical balance is reached and, depending on the orientation of the acceleration field, further increases in g can cause destabilization of the interface and reorientation of the fluid to a different and perhaps undesirable location within or outside of the container. The precise value of B at which such a reorientation might occur B_{cr} is an important design parameter for any capillarity-controlled fluid system and is particularly significant for fluids management and processes in space.

Duprez[19] and Maxwell[20] performed critical Bond-number analyses for confined geometries as early as the 1800s for the stability of pinned interfaces in circular and rectangular containers. These investigations are restricted to predominately flat surfaces originating out of an assumption of either a 90-deg contact angle θ condition or a pinned contact line. Treating θ as a parameter and allowing significant curvature of the interface, as is most common in capillary systems, solutions were obtained by Concus[21] for the right circular cylinder, Concus[22] for the infinite (i.e., two-dimensional) rectangular slot, and Seebold et al.[23] for the right circular annulus. The experimental works of Derdul et al.[24] and Masica et al.[25] concerning the cylinder and Labus[26] concerning the annulus are also noteworthy. Solutions for rotationally symmetric containers are given by Reynolds and Satterlee[27] and a number of solutions are reported for semibounded surfaces such as wall bound drops and bubbles by Reynolds and Satterlee,[27] pendant drops by Wente,[28] and liquid bridges by Coriell et al.[29] and Langbein.[30] Unbounded liquid layers are treated by Yiantsios and Higgins[31] with pertinent references contained therein.

[‡]Data available online at http://www.susqu.edu/facstaff/b/brakke.

A. Available Solutions

Useful numerical correlations for B_{cr} as a function of the contact angle can be gleaned from the work of Concus[21,22] and Seebold et al.[23] For the infinite slot one finds

$$B_{cr} \cong 0.71 + 1.74 \sin\theta \tag{1}$$

where B_{cr} is defined using the slot half-width, and for the right circular cylinder

$$B_{cr} \cong 0.81 + 2.59 \sin\theta \tag{2}$$

Larger values $B > B_{cr}$ lead to instability of the interface. Similar results for the annulus that depend heavily on the radius ratio R_i/R_o can be obtained. Using the form

$$B_{cr} \cong C_1 + C_2 \sin\theta \tag{3}$$

the annular interface correlation constants C_1 and C_2 are listed in Table 1. Note that B_{cr} is again defined on the outer radius R_o and that $R_i/R_o = 0$ in Eq. (3) recovers Eq. (2) for the right circular cylinder. Equations (1–3) show that B_{cr} is nonzero and positive for all values of the contact angle θ and solutions are symmetric about $\theta = 90$ deg.

The commonality between circular cylinders, slots, and annular containers is the smooth continuous boundary within which the fluids are confined. The situation differs significantly for a container with an interior corner of half angle α. As mathematically demonstrated by Concus and Finn[1] and just discussed, when $\theta < 90\,\text{deg} - \alpha$ (or $180\,\text{deg} > \theta > 180\,\text{deg} - \alpha$), hereafter referred to as the Concus–Finn condition, a critical wetting condition is established resulting in complete wetting of the corner by the fluid: the fluid is pumped into and along the interior corners of the container by capillary forces. Such surfaces are unconditionally unstable to adverse accelerations. Thus, for fluid-container systems satisfying the Concus–Finn condition $B_{cr} = 0$. Therefore, for problems such as the stability of a capillary surface in a rectangular container ($\alpha = 45$ deg) nonzero values for B_{cr} can only be obtained for contact angles in the range $45\,\text{deg} \le \theta \le 135$ deg. A sketch of several different interfacial regimes is provided in Fig. 6 for a container of square cross section.

Table 1 Correlation constants for circular annulus B_{cr}; Eq. (3)

R_i/R_o	C_1	C_2
0	0.81	2.59
0.1	1.30	1.99
0.25	1.83	0.83
0.5	0.22	1.39
0.75	0.28	1.01
1.0	0.74	0.41

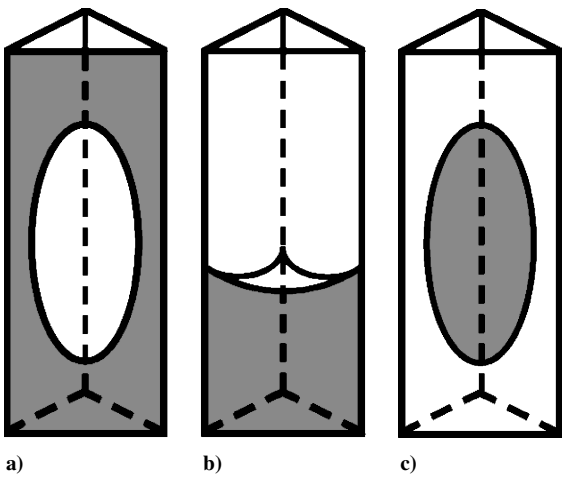

Fig. 6 Sketches to illustrate select wetting regimes in a right square cylinder. The cylinder is bisected along a diagonal that is in the plane of the page; the liquid phase is shaded. From Figs. 6a to 6c, $\theta \le 45$, $45\,\text{deg} < \theta < 135$, $135\,\text{deg} \le \theta$.

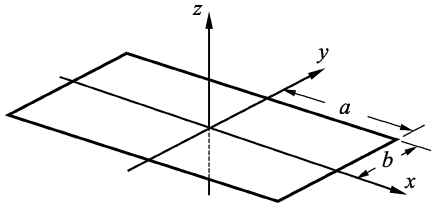

Fig. 7 Rectangular solution domain with the more dense fluid below the interface. Gravity acts positive in positive z direction.

The condition of Fig. 6b ($45\,\text{deg} < \theta < 135$ deg) is investigated here because the cases of Figs. 6a and 6c lack a finite-height single-valued equilibrium interface that spans the cylinder cross section. A more complete description of wetting regimes in containers with interior corners is provided by Langbein and Weislogel.[32]

Analytical solutions to such problems are only possible for the case $\theta \approx 90$ deg. For example, under this restriction, Maxwell[20] predicted the stability of an inverted capillary surface in a rectangular container of half-length a and half-width b. Figure 7 depicts this geometry, where the more dense fluid is below the interface and g acts positive in the positive z direction. Maxwell's solution is derived by minimizing the sum of surface and gravitational energies and assumes a pinned, predominately flat interface ($\theta \approx 90$ deg). His result is

$$B_{cr} = \rho g b^2/\sigma = (\pi^2/4)[1 + 4(b/a)^2] \tag{4}$$

where $0 < b/a \le 1$.

We extend Maxwell's solution method to the case of perfect slip at the contact line where θ is fixed at 90 deg. The result is

$$B_{cr} = \rho g b^2/\sigma = (\pi^2/4)[n^2 + (mb/a)^2] \tag{5}$$

where m and n identify the mode of the disturbance along the x and y directions, respectively; the perturbed surface is given by $z = \epsilon \cos(\pi m x/a)\cos(\pi n y/b)$, where $\epsilon \ll b$. Minimization of the energy requires $m = 1$, $n = 0$, leaving

$$B_{cr} = \rho g b^2/\sigma = (\pi^2/4)(b/a)^2 \tag{6}$$

which corrects a previously reported result by Weislogel and Hsieh.[33]

Comparison of Eqs. (4) and (6) shows that stability is enhanced by the pinned condition, as is commonly observed in practice. From Eq. (4), as $b/a \to 0$, $B_{cr} \to \pi^2/4$, which is equivalent to Eq. (1) with $\theta = 90$ deg, as well as to the solution for unbounded liquid layers,[30] where the disturbance wavelength is $\lambda = 4b$.

B. Advantages of Computing B_{cr} with SE

To account for significant variation in θ away from $\theta \approx 90$ deg, numerical solutions to idealized equations of fluid motion[21,23,33] were thought to be necessary. The governing second-order nonlinear partial differential equation is subject to the contact-angle condition along the container walls. The equation is linearized, and normal modes are introduced for the velocity potential and for a small perturbation to the leading-order static interface shape. The numerical approach requires solution of the resulting eigenvalue problem via the evaluation of the determinant of the solution matrix for the disturbance. A negative determinant implies growth of the disturbance and thus instability. For complex geometries as "benign" as the rectangular interface (Fig. 7), the computational effort using the preceding technique can be burdensome if not wasteful.

In contrast, the SE algorithm circumvents the intricacies of the preceding approach by iteratively computing surfaces in steps that eventually minimize the sum of surface and gravitational energies using a gradient-descent or conjugate-gradient method. The contact angle is implemented with constraint energy integrals defined for energy density of the wetted wall surfaces up to the contact line (see the mound example in the SE manual). Upon solution for the

equilibrium interface at a given Bond number (orientation and magnitude), a perturbation to the interface is added. The perturbation can be random spatially or can be specified exactly by the user. Stability of the perturbation is assessed either through a sign change of an eigenvalue, or, where the use of the "convex" property in SE for curved walls prohibits use of the "eigenprobe" command, by iteration until the perturbation diminishes or grows. Note that an iteration in SE is not a time step through the equations of motion for the fluids but rather one algorithmic step in a search for the static geometry that minimizes the sum of the energies defined by the user consistent with the geometrical constraints defined by the user. Based on stability of the first test, the Bond number is adjusted up or down, and the process repeated. Equilibrium surface solutions at unstable Bond numbers are found routinely, and thus the perturbation step is required. Some geometries are amenable to interrogation of the eigenvalues of the surface shape as demonstrated by Brakke for problems governed solely by the perimeter geometry[13] (i.e., fluid interfaces uninfluenced by contact angle and gravity). The eigenprobe method is generally quicker than the iteration method. In both methods the lower and upper bounds on B_{cr} can be found easily to better than one part in a thousand.

Grid convergence is assessed in the square container with pinned contact line. Table 2 shows that the error diminishes with increasing number of facets. This is consistent with a measure of geometric convergence shown for static equilibriums by Collicott.[34] Accuracy and computational time increase with the number of triangular facets in the model of the interface, which is controlled by the user. For reference, computation of all of the results in Table 2 required approximately one half-day of operator interaction with SE computations on a 600-MHz P-III machine.

C. Capillary Instability Validation

The two-dimensional infinite slot problem is defined as a two-dimensional model in SE instead of the three-dimensional model used for solving the cylindrical geometries. Computational time in this two-dimensional geometry is a matter of seconds, not minutes.

Table 3 presents the well-established B_{cr} results of Concus[21,22] for the two-dimensional slot and right circular cylinder for comparison to respective values computed using SE. The results agree to $\pm 0.5\%$ or better at $\theta = 90$ deg and 2.8% or better near $\theta = 0$ and serve as a benchmark for the SE stability analysis. The result for a pinned surface ($\theta \cong 90$ deg) in a right square cylinder is also listed in Table 3, which compares well with Maxwell's result, Eq. (4). For the case of $\theta = 90$ deg in a square container, B_{cr} is listed in Table 4 determined by Eq. (5) and SE for various modes m and n. The results agree within $\pm 1\%$ demonstrating that SE can also be used effectively to identify B_{cr} for at least some known modal disturbances other than the most unstable mode.

Solutions for B_{cr} in rectangular containers determined with SE are shown in Fig. 8 for aspect ratios ($b : a =$) 1, 1:2, 1:3, and 1:4 and contact angles θ in the admissible range 45 deg $\leq \theta \leq$ 135 deg. Correlation of these results in the traditional manner using the form $B_{cr} = D_1 + D_2 \sin\theta$ fails in this geometry for contact angles nearing the Concus–Finn condition. The numerical results of Concus[21,22] for the two-dimensional slot and the right circular cylinder are also provided in Fig. 8 via Eqs. (1) and (2), respectively. The SE calculations for the rectangular container are practical for $\theta = 47$ deg. Lower values approaching 45 deg can be solved by increasing grid resolution.

The rectangular geometry serves as a model for containers possessing interior corners. Such corners are commonly employed in fluids management systems in space.[35,36] The SE results reveal that, though stability is comparable to the infinite slot for large contact angles near 90 deg, the range of contact angles yielding positive values for the critical Bond number is significantly reduced as a result of a corner wetting phenomena governed by the Concus–Finn condition. B_{cr} is shown here to be $\mathcal{O}(1)$ for 45.6 deg $< \theta <$ 134.4 deg in a square cylinder, but diminishes to zero rapidly, if not discontinuously, as $\theta \to 45$ deg from above, or $\theta \to 135$ deg from below.

Validation in simple geometries permits extension of the method to more complex geometries. As a demonstration, in Fig. 9 is shown the surface mesh in a right cylinder of complex cross section that is solved for B_{cr} at $\theta = 60$ deg. This solution required approximately 1 min for grid refinement and 5 min to compute the equilibrium interface. Critical Bond number $B_{cr} = \rho g h^2/\sigma$, where h is the height of the letter, is found to be 2.06 ± 0.05 for $\theta = 60$ deg. The width of the structures in the letter is $w = 0.2h$, and 1066 facets describe the surface. The serif at the base of the letter is where the interface location tips up toward infinity for $B > B_{cr}$.

Table 2 Grid-convergence results[a]

Facets	B_{cr}	Difference from theory	% Error
64	13.555	1.217994	9.873
256	12.655	0.317994	2.578
1,024	12.415	0.077994	0.632
4,096	12.3525	0.015494	0.126
16,284	12.3375	0.000494	0.004
65,536	12.3375	0.000494	0.004

[a]The 16,284-facet case happened to work as well as the finer resolution case. This should be considered novel and not assumed in other work.

Table 4 B_{cr} in a rectangular (square) container: $\theta = 90$ deg, $b/a = 1$

(m, n)	B_{cr} [Eq. (5)]	B_{cr} (Evolver[a])
(1, 0)	2.467	2.47
(1, 1)	4.935	4.945
(2, 0)	9.869	9.945

[a]Data available online at http://www.susqu.edu/facstaff/ b/brakke.

Table 3 Benchmark B_{cr} results for SE[a]

Vessel geometry	θ, deg	B_{cr} (Concus[21,22])	B_{cr} (Evolver[b])	Difference, %
Infinite slot[c]	0.81	≈ 0.7346	0.755 ± 0.005	2.8
	90	2.4674	2.4675 ± 0.0005	0.5
Right circular cylinder[d]	8.11	1.175[d]	1.151 ± 0.001	−2
	90	3.39	3.393 ± 0.001	0.09
	90, pinned	14.67	14.7215	0.35
Right square cylinder[c]	90, pinned	12.33701	12.3375 ± 0.0005	0.004

[a]Free contact line condition is used unless otherwise specified. Equation (4) provides theoretical results for 90-deg pinned right square cylinder. Analytic solution for 90-deg pinned right circular cylinder given by Maxwell.[20]
[b]Data available online at http://www.susqu.edu/facstaff/b/brakke.
[c]Slot and square results based on eigenvalues.
[d]Circular results based on perturbations.
[e]Interpolated value from numerical results.

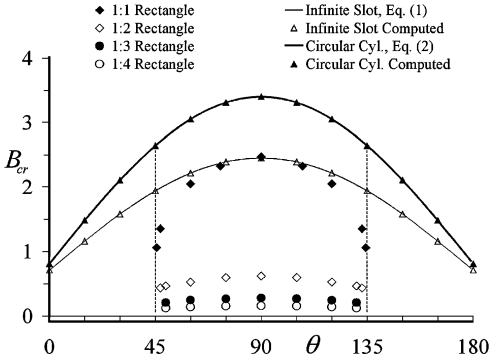

Fig. 8 SE computed critical Bond numbers vs contact angle (free contact line boundary condition) for rectangular cylinders of aspect ratios b/a = 1:1, 1:2, 1:3, and 1:4. Equations (1) and (2) for the infinite rectangular slot and right circular cylinder are provided for comparison.

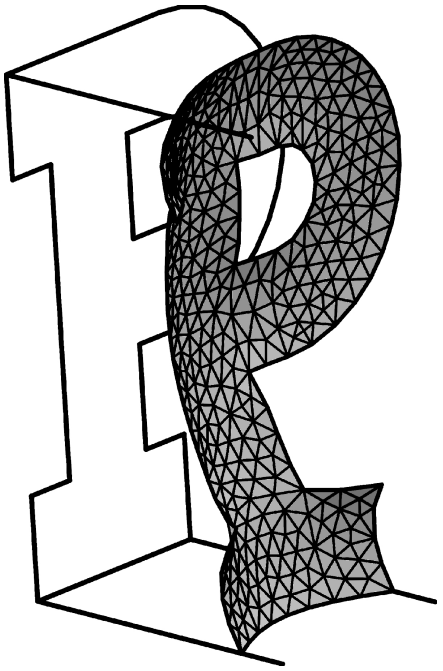

Fig. 9 Example of SE applied to capillary instability in a complex cylinder. Planform view of letter (left) with surface at $B_{cr} = 2.06$ with $\theta = 60$ deg computed (right). The interface becomes unstable first at the base of the letter.

IV. Conclusions

The surface evolver (SE) code can be applied to solve for Concus–Finn critical contact angles when a small finite inaccuracy is tolerable. The inaccuracy is not a flaw in SE but an artifact of the discretization of the surface and finite memory and compute time. A method is described for such computations and is validated against theory, including corner bluntness effects. Three conditions for valid solutions are recommended: approximately 10^3 faces per corner, use of automated edge length limits, and growth of the interface height less than one part per million per iteration following an iteration count 10 times the total face count.

Accuracy of the critical contact-angle solution depends on the number of faces used in the interface, with the error for the discretized surfaces favoring existence of a finite-height single-valued solution. Demonstration that SE can capture the distinction between the two classes of solutions considered in Concus–Finn theory, in addition to already demonstrated capabilities of SE, increases confidence in the use of SE for design and analysis of low-g two-phase fluid systems.

The SE algorithm is demonstrated additionally as an accurate and useful tool for predicting the onset of the Rayleigh–Taylor interfacial instability. The significant advantage of using SE compared to other numerical techniques lies in the speed and facility with which complex geometries can be coded and solved. Discretized capillary interfaces are found to be slightly more stable than the true continuous surfaces they model. However, by increasing the number of facets (and hence, compute time) precision of 0.004% has been demonstrated for critical Bond number. The work is not exhaustive, and some powerful features and procedures in SE remain unexploited for these applications.

Acknowledgments

M. Weislogel is supported in part under NASA Contract NAS3-00126. Discussions with Paul Concus were instrumental in this effort.

References

[1]Concus, P., and Finn, R., "On the Behavior of a Capillary Free Surface in a Wedge," *Proceedings of the National Academy of Sciences of the United States of America*, Vol. 63, No. 2, 1969, pp. 292–299.

[2]Princen, H. M., "Capillary Phenomena in Assemblies of Parallel Cylinders I: Capillary Rise Between Two Cylinders," *Journal of Colloidal and Interface Science*, Vol. 30, No. 1, 1969, pp. 69–75.

[3]Myshkis, A. D., Babskii, V. G., Kopachevshii, N. D., Slobozhanin, L. A., and Tyuptsov, A. D., *Low-Gravity Fluid Mechanics*, Springer-Verlag, Berlin, 1987.

[4]Mittelmann, H. D., and Zhu, A., "Capillary Surfaces with Different Contact Angles in a Corner," *Microgravity Science and Technology*, Vol. 9, Aug. 1996, pp. 22–27.

[5]Langbein, D., *Capillary Surfaces–Shape, Stability, Dynamics, in Particular Under Weightlessness*, Springer-Verlag, Berlin, 2002, Chap. 8.

[6]Concus, P., and Finn, R., "Dichotomous Behavior of Capillary Surfaces in Zero Gravity," *Microgravity Science and Technology*, Vol. 3, No. 2, 1990, pp. 87–92.

[7]Smedley, G., "Containments for Liquids at Zero Gravity," *Microgravity Science and Technology*, Vol. 3, May 1990, pp. 13–23.

[8]Concus, P., and Finn, R., "Capillary Surfaces in a Wedge—Differing Contact Angles," *Microgravity Science and Technology*, Vol. 7, No. 2, 1994, pp. 152–155.

[9]Chen, Y., and Collicott, S. H., "Investigation of the Wetting Behavior of a Vane-Wall Gap in Propellant Tanks," AIAA Paper 2002-3986, July 2002.

[10]Concus, P., Finn, R., and Weislogel, M., "Measurement of Critical Contact Angle in a Microgravity Space Experiment," *Experiments in Fluids*, Vol. 28, No. 3, 2000, pp. 197–205.

[11]Smedley, G., "Preliminary Drop-Tower Experiments on Liquid-Interface Geometry in Partially Filled Containers at Zero-Gravity," *Experiments in Fluids*, Vol. 8, March 1990, pp. 312–318.

[12]Finn, R., "Capillary Surface Interfaces," *Notices of the AMS*, Vol. 46, No. 7, 1999, pp. 770–781.

[13]Brakke, K. A., "The Surface Evolver and the Stability of Liquid Surfaces," *Philosophical Transactions of the Royal Society of London*, Vol. 354, 1996, pp. 2143–2157.

[14]Brakke, K. A., "The Surface Evolver," *Experimental Mathematics*, Vol. 1, No. 2, 1992, pp. 141–165.

[15]Bayt, R. L., and Collicott, S. H., "Effects of an Elliptic End-Cap on the Ullage Bubble Stability in the Gravity Probe-B Satellite," AIAA Paper 96-0596, Jan. 1996.

[16]Tegart, J., "A Vane-Type Propellant Management Device," AIAA Paper 97-3028, July 1997.

[17]Ambrose, J., Yendler, B., and Collicott, S. H., "Modeling to Evaluate a Spacecraft Propellant Gauging System," *Journal of Spacecraft and Rockets*, Vol. 37, No. 6, 2000, pp. 833–835.

[18]National Research Council-Space Studies Board, "Microgravity Research in Support of Technologies for the Human Exploration and Development of Space and Planetary Bodeis," National Academic Press, Technical Rept., Washington, DC, 2000.

[19]Duprez, M., "Sur un cas Particularier 1 Equilibre des Liquids," *Nouveaux Mem. De l'Acad. De Belquique*, 1854.

[20]Maxwell, J. C., "Capillary Action," *Scientific Papers of James Clerk Maxwell*, Cambridge Univ. Press, London, 1890.

[21]Concus, P., "Static Menisci in a Vertical Right Circular Cylinder," *Journal of Fluid Mechanics*, Vol. 34, No. 3, 1968, pp. 481–495.

[22]Concus, P., "Capillary Stability in an Inverted Rectangular Channel for Free Surfaces with Curvature of Changing Sign," *AIAA Journal*, Vol. 2, No. 12, 1964, pp. 2228–2230.

[23]Seebold, J. G., Hollister, M. P., and Satterlee, H. P., "Capillary Hydrostatics in Annular Tanks," *Journal of Spacecraft and Rockets*, Vol. 4, No. 1, 1967, pp. 101–105.

[24]Derdul, J. D., Masica, W. J., and Petrash, D. A., "Hydrostatic Stability of the Liquid-Vapor Interface in a Low-Acceleration Field," NASA TN D-2444, Aug. 1964.
[25]Masica, W. J., Otto, E. W., and Petrash, D. A., "Hydrostatic Stability of the Liquid-Vapor Interface in a Gravitational Field," NASA TN D-2267, May 1964.
[26]Labus, T. L., "Natural Frequency of Liquids in Annular Cylinders Under Low Gravity Conditions," NASA TN D-5412, Sept. 1969.
[27]Reynolds, W. C., and Satterlee, H. M., "Liquid Propellant Behavior at Low and Zero g," *The Dynamic Behavior of Liquids*, edited by H. N. Abramson, NASA SP-106, 1966, pp. 387–440.
[28]Wente, H. C., "The Stability of the Axially Symmetric Pedant Drop," *Pacific Journal of Mathematics*, Vol. 88, No. 2, 1980, pp. 421–470.
[29]Coriell, S. R., Hardy, S. C., and Cordes, M. R., "Stability of Liquid Zones," *Journal Colloid and Interfacial Science*, Vol. 60, No. 1, 1977, pp. 126–136.
[30]Langbein, D., "Stability of Liquid Bridges Between Parallel Plates," *Microgravity Science and Technology*, Vol. 5, 1992, pp. 2–11.
[31]Yiantsios, S. G., and Higgins, B. G., "Rayleigh-Taylor Instability in Thin Viscous Films," *Physics of Fluids A*, Vol. 1, Sept. 1989, pp. 1484–1501.
[32]Langbein, D., and Weislogel, M. M., "Dynamics of Liquids in Edges and Corners (DYLCO): IML-2 Experiment for the BDPU," NASA TM 1998-207916, Aug. 1998.
[33]Weislogel, M. M., and Hsieh, K. C., "Stability of a Capillary Surface in a Rectangular Container," NASA TM-1998-206629, Jan. 1998.
[34]Collicott, S. H., "Convergence Behavior of Surface Evolver Applied to a Generic Propellant Management Device," *Journal of Propulsion and Power*, Vol. 17, No. 4, 2001, pp. 845–851.
[35]Jaekle, D. E., Jr., "Propellant Management Device Conceptual Design and Analysis—Sponges," AIAA Paper 93-1970, June 1993.
[36]Jaekle, D. E., Jr., "Propellant Management Device Conceptual Design and Analysis—Vanes," AIAA Paper 91-2172, July 1991.

S. K. Aggarwal
Associate Editor